Dynamics of lock-release crystalline gravity currents

M. D. Sharifuzzaman, Charles J. Lemckert & Amir Etemad-Shahidi

Submit your article to this journal 🗗

View related articles 🗗

View Crossmark data 🗗

INWASCON

Taylor & Francis
Taylor & Francis Group

OPEN ACCESS   Check for updates

Dynamics of lock-release crystalline gravity currents

M. D. Sharifuzzaman[a], Charles J. Lemckert[b] and Amir Etemad-Shahidi[a]

[a]Griffith School of Engineering, Griffith University, Griffith, Australia; [b]Faculty of Arts and Design, University of Canberra, Canberra, Australia

ABSTRACT

Coastal and marine environments are impacted by inflows of varying types and chemical compositions. This novel study experimentally investigated the dynamics of a particular type of inflow—crystalline gravity currents (CGC) produced by the lock release of over-saturated brine solutions (i.e., they contain a proportion of suspended salt crystals) into a non-stratified ambient. Such flows may occur from desalination and chemical plant discharges. CGCs were found to show two distinguishing characteristics from normal under-saturated gravity currents (UGC). One was that CGCs have longer slumping distances than UGC while the other was that during the self-similar phase, CGCs have a decreasing trend in their velocities, and the current's height is no longer constant. These differences result because the CGCs drop crystals onto the bed as they advance. Their flow behaviour was also found to be dependent on the flow head density or local density; whereas, UGC flow is a function of the initial fluid density. This unique study gives a significant insight into crystalline gravity currents showing how they can impact the coastal environments they are encountered in, e.g., the discharge vicinity of desalination and chemical plants.

1. Introduction

Gravity currents, which are also known as density currents, are established when one fluid flows into another with different density, and the flows are driven by their density difference. These very common and important phenomena occur within numerous natural and constructed systems, including the heating and cooling of rooms (23) in water treatment plant clarifiers (19), in reservoir destratification systems (Lemckert & Imberger, 15, 16), and in the operation of water regulating lock structures designed to modify and control estuarine and lake systems (17; 30; 31). These currents are also relevant to engineering sciences such as in industrial safety and environmental protection. A common method of creating gravity currents in the laboratory is by quickly removing a vertical barrier (lock) separating two fluids of different densities in a channel. Using this technique and with salt water and fresh water solutions as the fluids, many researchers have conducted lock release gravity current experiments to understand their fundamental behaviour (1; 4; 5; 8; 12; 14; 17; 20; 22; 24; 26; 28). However, crystalline gravity currents have not been studied extensively yet, and there is very little fundamental knowledge of their behaviour. Crystalline gravity currents are suspensions of dense particles that spread into an ambient fluid due to the difference in the density of the suspension and that of the ambient fluid. During the evolution of the crystalline gravity current, the particles

continually dissolve, thus reducing the excess density of suspension and therefore reducing the driving buoyancy force.

The UGC has different physical phases across their propagation (8). The first is the initial slumping phase (Figure 1, panels' b–e). During this, the front of the gravity current, which is known as the head, moves with a constant speed (U) and maintains nearly constant depth (h) (8). After the first phase, the head collapses (Figure 1 panel f). At slumping distance (X_s), the head becomes well-formed because the reflective wave catches up with the front thus giving its characteristic inertial semicircular cross section. This phase is known as self-similar phase (24).

Here, the theoretical slumping distance is defined by (24) –

$$X_s = x_0 \left(3 + 7.4 \frac{h}{H} \right) \tag{1}$$

where, x_0 = lock length, h = height of the head of the gravity current from the bed and H = initial height of water, which is same as the height of lock fluid in this study.

After this self-similar stage, even though the head was continuously entraining ambient fluid, its volume decreases with downstream distance due to the mixed fluid being left behind in the tail (Figure 1 panels' g to k).
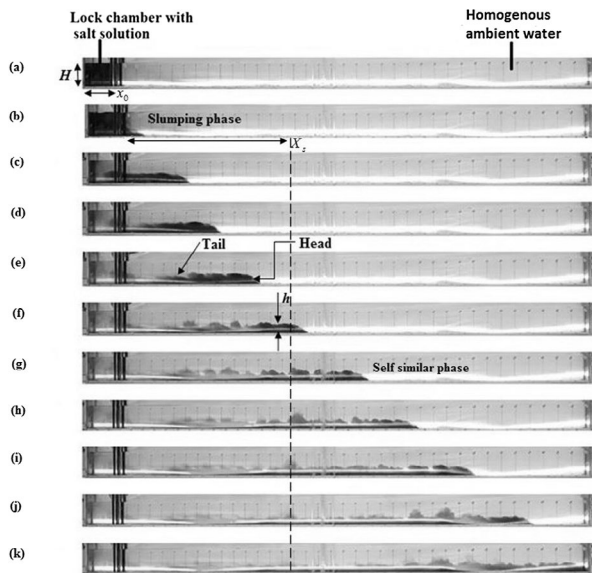
Figure 1. Phases of a lock-release gravity current (following the style of 8) (the non-uniform white streak is due to the LED backlighting and the crippled baking paper in front of the LED strip, this did not affect the data analysis).

The third phase may be reached if the flow continues far enough when the viscous effects are dominant, which means low Reynold's number (Re) (27). The Reynolds number can be defined as $Re = UR_h/\nu$, where, R_h = hydraulic radius in m; ν = viscosity of the fluid in m^2s^{-1}. For a rectangular cross-section channel, the hydraulic radius can be calculated by R_h = Area / Wetted perimeter = $Bh/ (B + 2\,h)$. Here, B = width of the tank in m.

During the current's progress, several studies have found the most significant feature of shallow water gravity current is the uniformity of the densimetric Froude number (F_d), based on initial flow conditions, and it can be defined as

$$F_d = \frac{U}{\sqrt{g'H}} \qquad (2)$$

where, g' is the reduced gravity and can be defined as

$$g' = g\frac{\rho_1 - \rho_0}{\rho_0} \qquad (3)$$

Here, ρ_1 = lock fluid density in kgm^{-3}, ρ_0 = ambient water density in kgm^{-3} and g = acceleration due to gravity in ms^{-2}.

Using an extensive array of laboratory experiments, 1 found that for a rectangular lock and channel, F_d is 0.46, while 7 obtained 0.456, and 14 derived 0.41 from detailed laser Doppler anemometry (LDA) measurements. The differing values of F_d appear to arise from the scale of the experiments, which influence the mixing between the two fluids and the gravity current Re and this scale feature had been found to be important

in describing the mixing that occurs within the gravity current flow (Hartel, Carlsson, & Thunblom, 9; 6; Hartel, Meiburg, & Necker, 10; 11; 14).

Apart from the normal and crystalline gravity current, there is another type, which is turbidity current which has received extensive attention from researchers (18; 21; 25; 27). These gravity currents, where the increase in density of the gravity current is due to non-dissolving particles (possible salinity and temperature differences), are often referred to as particle-driven gravity currents or suspension flows. However, the behaviour of turbidity currents can be very similar to gravity currents caused by dissolved materials if the suspended material is very fine and rate of fallout is small (27).

There is a profound scarcity of research regarding the effect of the presence of dissolving salt crystals in the initiation and behaviour of *CGC*. The work presented in this paper is focused on the dynamics of crystalline gravity currents generated through the lock-exchange approach. Salt crystals of two different sizes were used (L—average diameter 0.73 mm and S—average diameter 0.51 mm) with solutions used up to a supersaturated state. This paper comprises an introduction, and then related theories and research findings from previous studies are discussed. After that, the methodology and finally, the results and discussions are outlined—followed by the conclusions.

2. Materials and method

The lock release experiments were conducted in a flume made of Plexiglas with a smooth horizontal bed. The flume was a 4 m × 0.1 m × 0.3 m rectangular cross section tank. The lock chamber dimension was 0.235 m × 0.1 m × 0.3 m. The front of the tank was marked at 20 equal interval points. A schematic of the flume is presented in Figure 2.

The back wall of the flume was fitted with baking paper, and behind that, a LED SMD-5050 strip with 12 V power supply was attached to a frame for the backlighting purpose. The salt water mixture was prepared and mixed separately in a bucket with a paint mixer attached to a drill, and dye was added at the end to make the solution opaque. The lock chamber was filled with the saline solution while the rest of the tank was filled with fresh homogenous water; both sides were filled up to the same depth of 20 cm (H), which was true for all the experiments conducted in this study. Two different sizes of salt crystals were used for comparison purposes—larger particle L (600 μm to 1.18 mm, average size 0.73 mm) and smaller particle S (425 μm to 600 μm, average size 0.51 mm). Raw salt crystals were sieved to obtain the needed amount for each experiment. The temperature was measured using a thermometer and was used to estimate the density and kinematic viscosity of the fresh water. For measuring the density of the unsaturated lock fluid, hydrometers was used, and for over-saturated lock
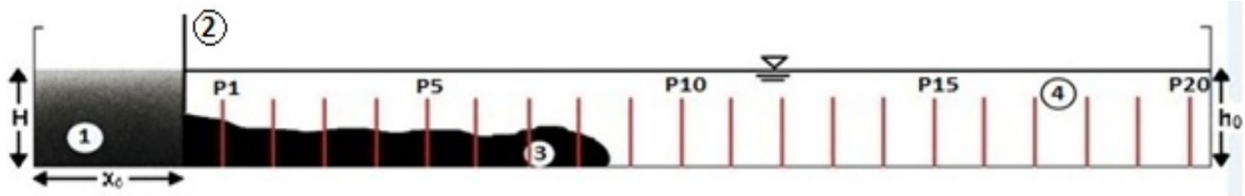
Figure 2. Schematic of the lock release flume. 1: high-density lock solution, 2: lock gate, 3: gravity current formed due to lock-gate removal, 4: freshwater and P1, P5, P10 and P20 are equally distanced marked points.

fluid, the density was calculated by the mass balance method with a 3% error. The propagation of gravity currents was monitored and recorded by a video camera at 60fps, and the footage was then analysed using a media player with high-precision timing enabled. In total 33, experimental runs were conducted in this study (each replicated twice).

3. Results and discussion

Several lock release experiments were conducted using lock solutions of varying density. The following Tables 1–3 summarize the parameters of the experiments conducted in this work. In the tables, the theoretical slumping distance (X_{st}) from Equation (1), the experimentally derived slumping distance (X_{sp}) and other flow characteristics are shown for each test.

Tables 2 and 3 contain the data for *CGC* experiments. The former contains data for L crystals, and the later comprises the data for S crystals.

Table 4 shows the overall and local F_d data for both L and S crystals.

Examples of the velocity vs. distance data from three experiments are given in Figure 3. The velocity was measured at 20 equal distance points, i.e., after the lock gate was removed, the current was allowed to progress through 18.65 cm before it reached the first marked point, which is the reason for the lines not starting from when the distance is zero. As seen, right after removing the gate, there is a gradual increase in the starting velocity of the *UGC* whereas, for *CGC*, velocity shows a decreasing trend for both L and S.

Figure 3 shows that this gradual increase in starting velocity exists until 0.6 m from the lock gate for the *UGC* whereas, for *CGC*, negligible fluctuation in velocity is observed until 1.5 m distance from the lock gate for particle L and until 2 m for particle S. The slight fluctuation on velocities maybe due to the fact that they were measured at points of an equal interval from each other and the velocities of flow in between two points is not recorded. The self-similar phase occurs after the head of the gravity current had advanced about 8 to 10 lock lengths for the unsaturated solution (24), which is also true for up to 300 g salt/L. However, for other unsaturated solutions having lower salt concentration, the slumping distance is shorter than what 24 had found in their study. Furthermore, the *UGC* showed an initial

Table 1. Experimental conditions and other characteristics of experiments (*UGC*).

Salt conc. (gL^{-1})	X_{st} (m)	X_{sp} (m)	ρ_1 (kgm^{-3})	ρ_0 (kgm^{-3})	F_d	U (ms^{-1})	Re
30	1.34	1.67	1019	997.42	0.38	0.08	2696
60	1.36	2.23	1041	997.42	0.37	0.11	3558
90	1.36	1.86	1057	998.1	0.39	0.13	4514
120	1.33	2.23	1075	997.42	0.38	0.15	5026
150	1.36	1.67	1080	997.42	0.41	0.17	5576
180	1.36	2.05	1110	998.1	0.38	0.18	6203
210	1.35	1.86	1123	997.42	0.39	0.19	6597
240	1.36	2.05	1147	998.1	0.38	0.20	6906
270	1.35	2.05	1159	997.42	0.39	0.22	7342
300	1.37	1.68	1172	997.42	0.40	0.23	7717

Table 2. Experimental conditions and other characteristics of experiments (*CGC* with L crystals).

Salt conc. (gL^{-1})	X_{st} (m)	X_{sp} (m)	ρ_1 (kgm^{-3})	ρ_0 (kgm^{-3})	F_d	U (ms^{-1})	Re
340	1.27	1.68	1181	998.1	0.41	0.23	7541
370	1.25	1.68	1192	998.1	0.38	0.23	7300
400	1.17	1.86	1203	998.1	0.39	0.25	7104
430	1.25	1.86	1214	998.1	0.36	0.23	7395
460	1.33	1.86	1224.5	998.1	0.37	0.25	7924
490	1.32	1.68	1234	998.1	0.35	0.24	8018
520	1.30	1.68	1244	998.1	0.34	0.24	8041
550	1.31	2.05	1253	998.1	0.36	0.25	8446
580	1.40	1.86	1263	998.1	0.33	0.23	8011
610	1.31	2.24	1273	998.1	0.33	0.24	8259
640	1.29	1.68	1281	998.1	0.31	0.23	8109
670	1.30	1.68	1290	998.1	0.32	0.24	8321
700	1.30	1.31	1298.5	997.42	0.30	0.23	8314
730	1.27	1.31	1307	997.42	0.29	0.23	8274
760	1.27	1.31	1316	997.42	0.29	0.23	8412
790	1.26	1.31	1323	997.42	0.27	0.22	7905
820	1.26	1.31	1331	997.42	0.26	0.22	8042
850	1.26	1.49	1339	997.42	0.28	0.24	8483
880	1.23	1.31	1347.01	997.42	0.27	0.23	8473

Table 3. Experimental conditions and other characteristics of experiments (*CGC* with S crystals).

Salt conc. (gL^{-1})	X_{st} (m)	X_{sp} (m)	ρ_1 (kgm^{-3})	ρ_0 (kgm^{-3})	F_d	U (ms^{-1})	Re
340	1.5	1.68	1210	997.05	0.38	0.25	8898
520	1.46	2.6	1288	997.05	0.35	0.27	9457
610	1.46	2.05	1310	998.31	0.36	0.28	8742
700	1.44	1.49	1330	997.05	0.34	0.27	9620

increase in velocity right after the removal of the lock gate followed by an increasing trend until self-similar phase started whereas, *CGC* (both L and S) showed a decreasing trend in velocity from the start. The initial

velocity of *CGC* for all densities is much higher than *UGC*. The gravity current containing fewer suspended salt crystals such as 340 g/L and 400 g/L solutions showed an increase in velocity in the early stages of advancement until 1.5 m. On the other hand, currents containing larger masses of suspended salt crystals were more likely to exhibit a decrease in the velocity after passing 2 m distance. After passing 2 m, gravity current for all densities showed a continual decrease in velocity. This deceleration was more dramatic for the over-saturated suspended gravity currents. This behaviour of gravity current is expected and is in good agreement with previous studies (1; 7; Hartel et al., 10; 13; 14; 26; 29) as this marks the near-constant velocity slumping phase. Then, as the inertial forces became dominant, the velocity started to decrease.

In order to investigate whether or not traditional gravity currents are different to crystalline gravity currents, the F_d pattern was also examined alongside with slumping distance. F_d was calculated using Equation (2) and plotted against the density ratio (ratio of lock fluid density to ambient water density) in Figure 4.

F_d for particle S is also plotted on the same graph for easier comparison, and it is observed that for smaller size particles, F_d has higher values than particle L. When smaller particles are in the current, they suspend for longer than bigger particles. Large crystals tend to settle very quickly and hence reduce the density of the gravity current, whereas, particle S being smaller remains suspended in the current for a longer duration. In doing so, the driving density difference between the two solution remains higher, which explains why F_d for particle S solutions is larger than those of particle L solutions (salt concentration of 340, 520, 610, and 700 gL^{-1}). For two particle L (820 and 880g salt/L) solutions, F_d was found to be 5% higher than particle S value. One explanation for this could be parallax error while recording the video footage, sudden shake in the slider caused hindrance in the recording, which later contributed to the 5% error in reading the h of the gravity current. The local density F_d was calculated following Equation (2) from h instead of H for both crystal sizes (L and S) in saturated salt solution and plotted in Figure 4 to show a direct comparison. From this, it can be seen that the *CGC*, after a certain time that is required to dump all the suspended salt crystals, behaves like a normal gravity current and entirely forgets the presence of crystals. It maintains a steady F_d throughout the entire self-similar phase afterward. It also means that the initial flow conditions do not contribute to the behaviour of the crystalline gravity current after all the particles had settled down. Only the local effect then governs its behaviour. The mean of F_d for *CGC* and *UGC* showed a difference in values, which can be merited to the presence of salt crystals, which contributes to the driving force of the currents. The reason for the mean F_d of unsaturated current being lower than *CGC* is that there are no salt crystals inside the current, which make the density lower than *CGC* and hence reduces the F_d.

17 noted that F_d varies (0.40–0.53) as a result of the scale of the experiment as this influences the mixing between the two fluids and the gravity current *Re*. This

Table 4. Overall and local F_d For *CGC* with L and S crystals.

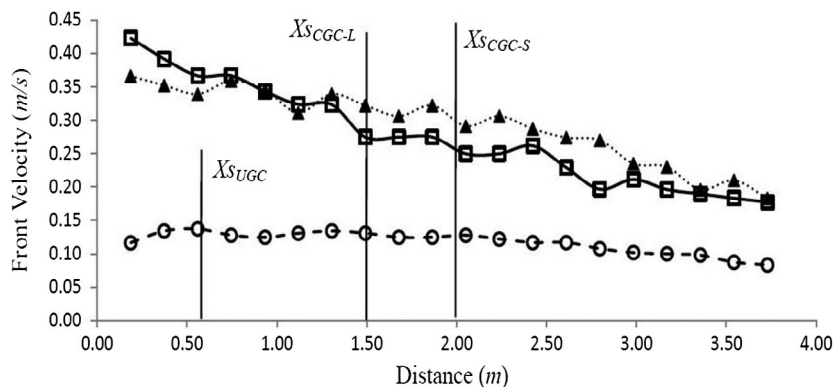| Density ratio	Overall F_d for L crystals	Local F_d for L crystals	Overall F_d for S crystals	Local F_d for S crystals
1.18	0.397	0.44		
1.19	0.375	0.43		
1.21	0.391	0.45		
1.22	0.357	0.43		
1.23	0.374	0.45	0.347	0.42
1.24	0.348	0.45		
1.25	0.339	0.45		
1.26	0.358	0.47		
1.27	0.326	0.44		
1.275	0.328	0.46		
1.285	0.309	0.46		
1.29	0.319	0.47		
1.30	0.299	0.46	0.315	0.44
1.31	0.295	0.47		
1.32	0.294	0.47	0.294	0.47
1.326	0.276	0.46		
1.334	0.268	0.46		
1.34	0.289	0.45	0.294	0.45
1.35	0.279	0.44		

Figure 3. Average front velocity vs. distance—circles are for unsaturated gravity currents, squares are for over-saturated crystalline gravity currents (L) and blocked triangles are representing over-saturated crystalline gravity currents (S).
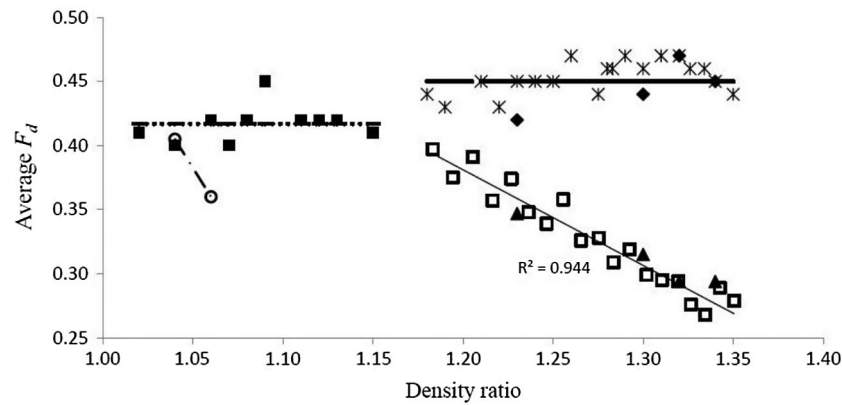
Figure 4. Non-dimensional F_d vs. density ratio for *CGC*'s self-similar phase (hollow rectangles are data from experiments for particle L, blocked triangles are data from experiments for particle S; hollow circles are data in similar experimental conditions extracted from (3; 14) sediment-laden flow), X's are local F_d calculated from settling velocity data for Particle L, blocked rectangles are local F_d calculated from settling velocity data for Particle S and the blocked squares are for *UGC*.

is in agreement with the literature [e.g., 1, 7, 10, 15, 16, 17, 25, 30, and 33]. Data extracted for sediment-laden gravity currents (3; 15) under similar experimental conditions as this study shows that the values for F_d lie below what was found here. This shows an important feature of crystalline gravity currents and its difference from sediment-laden currents. The average F_d leading up to supersaturation meets with expected values as discussed by 2. The energy conservation theory discussed in 2 paper predicts that the Froude number will be about 0.5 regardless of the Reynolds number of the flow, with 12 finding that this value could fluctuate from 0.42 to 0.48 at low and high *Re,* respectively. Figure 4 shows a good agreement and relationship between F_d and density ratio when the *CGC* is in the self-similar phase. As it can be seen from figure 3, the front velocity decreases gradually after the observed slumping distance due to mixing and entrainment (27), which changes the density and slows down the front, therefore the merit for decreasing F_d can be given to this factor. From this relationship, F_d can be easily obtained for any given density ratio to know if the flow is subcritical or not.

4. Conclusions

The dynamics of lock release crystalline gravity currents containing suspended salt crystals were studied experimentally. The results were compared with those of unsaturated brine gravity currents under similar experimental conditions. Data were also extracted from the literature for sediment-laden lock release gravity currents and compared to the findings from this study focusing on the self-similar or constant speed phase.

It was found that the slumping distances of *UGC*s are shorter than those of *CGC*s. This is due to the fact that when *CGC*s are created, their initial densities are much higher than *UGC*s and therefore, their velocities are also higher. As a result of which, the reflective bore required

considerably longer time to catch up with the current head of a *CGC*. For the conditions used in this study, the theoretical and experimental slumping distance data show that the experimental values are always higher than the theoretical slumping distances.

The non-dimensional F_d showed a good relationship with the density ratio for *CGC*s. F_d followed a decreasing trend with a high correlation coefficient of 0.944 for L crystals and 0.810 for S crystals with the increase of the density ratio from 1.18 to 1.41 focused in the self-similar phase. However, F_d for *UGC* remains almost similar (0.37 to 0.41) while data extracted from sediment-laden flow show a more or less similar trend to that of *CGC*. This feature shows the fundamental difference between crystalline and non-crystalline gravity currents including sediment-laden ones. Another significant finding was that initial flow conditions do not contribute to the behaviour of the crystalline gravity current after that all crystals have settled down. In other words, only the local effects govern its behaviour, not the initial flow characteristics. A difference was also observed in slumping distance and the start of the self-similar phase. In *UGC,* it was 0.6 m from the lock gate whereas for the over-saturated suspended salt gravity currents, slumping phase finished at 1.5 m from the lock gate (particle L) and at 2 m for particle S, which is logical because smaller crystals stay suspended for a longer time thereby accounts for the excess density difference. In addition, the non-crystalline gravity current showed an initial increase in velocity right after the removal of the lock gate followed by an increasing trend until self-similar phase started whereas, crystalline (both L and S) flows showed a decreasing trend in velocity from the start.

The outcomes of this experimental study showed that dynamics of crystalline gravity currents are quite different from those of unsaturated. The temporal change in the driving buoyancy affects the velocity. The results of this study can be used to improve guidelines to ensure that salinity levels after desalination discharge are

minimized to reduce environmental harm. The growing demand for a safe and reliable water supply has resulted in the construction and/or proposal of numerous desalination plants. Each plant requires the disposal of saline brines that may have adverse effects on the environment should the plants be overloaded and the brine solution not fully dissolved before entering the natural environment. However, their operation is essential, particularly in times of drought.

Disclosure statement

No potential conflict of interest was reported by the authors.

References

Barr, D. I. H. (1967). Densimetric exchange flows in rectangular channels III – Large scale experiments. *Houille Blanche, 6*, 619–631.

Benjamin, T. B. (1968). Gravity currents and related phenomena. *Journal of Fluid Mechanics, 31*, 209–248.

Best, J. L., Kirkbride, A. D., & Peakall, J. (2001). Mean flow and turbulence structure of sediment-laden gravity currents: New insights using ultrasonic doppler velocity profiling. In W. McCaffrey, B. Kneller, & J. Peakall (Eds.), *Particulate gravity currents* (Vol. 31, pp. 159–172). Oxford, UK: Blackwell Publishing Limited. Special Publication of the International Association of Sedimentologists.

Birman, V. K., Battandier, B. A., Meiburg, E., & Linden, P. F. (2007). Lock exchange flows in sloping channels. *Journal of Fluid Mechanics, 577*, 53–77.

Garcia, M. H. (1993). Hydraulic jumps in sediment-driven bottom currents. *Journal of Hydraulic Engineering, 119*(10), 1094–1117.

Garcia, M. H., & Parsons, J. D. (1996). Mixing at the front of gravity currents. *Dynamics of Atmosphere and Oceans, 24*(1–4), 197–205.

Hacker, J., Linden, P. F., & Dalziel, S. B. (1996). Mixing in lock release gravity currents. *Dynamics of Atmosphere and Oceans, 24*(1–4), 183–195.

Hallworth, M. A., Philips, J. C., Huppert, H. E., & Sparks, R. S. J. (1996). Entrainment into two-dimensional and axisymmetric turbulent gravity currents. *Journal of Fluid Mechanics, 308*, 289–311.

Hartel, C., Meiburg, E., & Necker, F. (1999). Vorticity dynamics during the startup phase of gravity currents. *II NuovoCimento, 22*(6), 823–833.

Hartel, C., Carlsson, F., & Thunblom, M. (2000). Analysis and direct numerical simulation of the flow at a gravity current head. Part 2. The lobe and cleft instability. *Journal of Fluid Mechanics, 418*, 213–229.

Huq, P. (1996). The role of aspect ratio on entrainment rates of instantaneous, axisymmetric finite volume releases of dense fluid. *Journal of Hazardous Materials, 49*, 89–101.

Keulegan, G. H. (1957). An experimental study of the motion of saline water from locks into fresh water channels.

Kneller, B. C., Bennet, S. J., & McCaffery, W. D. (1997). Velocity and turbulence structure of gravity currents and internal solitary waves: Potential sediment transport and the formation of wave ripples in deep water. *Journal of Sedimentary Geology, 112*(3), 235–250.

Kneller, B. C., Bennet, S. J., & McCaffery, W. D. (1999). Velocity structure, turbulence and fluid stresses in experimental gravity currents. *Journal of Geophysical Research, 104*(C3), 5381–5391.

Lemckert, C. J., & Imberger, J. (1993a). Energetic bubble plumes in arbitrary stratification. *Journal of Hydraulic Engineering, 119*(6), 680–703.

Lemckert, C. J., & Imberger, J. (1993b). Axisymmetric intrusive gravity currents in stratified reservoirs. *Journal of Hydraulic Engineering, 119*(6), 662–679.

Lemckert, C. J., Taylor, B., & Schacht, C. (2002). Initial spreading behavior of water released from a swinging gate lock. *Journal of Coastal Research, 36*, 450–458.

Lowe, D. R. (1982). Sediment gravity flows: II. Depositional models with special reference to the deposits of high density turbidity currents. *Journal of Sedimentary Research, 52*(1), 279–297.

Marle, C. V., & Kranenburg, C. (1994). Effects of gravity current in circular secondary clarifiers. *Journal of Environmental Engineering, 120*(4), 943–960.

Marleau, J. L., Flynn, M. R., & Sutherland, B. R. (2015). Gravity currents propagating up a slope in a two layer fluid. *Physics of Fluids, 27*, 036601–036617.

Middleton, G. V., & Hampton, M. A. (1973). Sediment gravity flows: Mechanisms of flow and deposition. *Turbidities and Deep Water Sedimentation. Short course notes* (pp. 1–38). Los Angeles, CA: SEPM (Pacific section).

Nogueira, H. I. S., Claudia, A., Eksa, A., & Mario, J. F. (2013). Analysis of lock-exchange gravity currents over smooth and rough beds. *Journal of Hydraulic Research, 51*(4), 417–431.

Rees, S. J., McGuirk, J. J., & Haves, P. (2001). Numerical investigation of transient buoyant flow in a room with displacement ventilation and chilled ceiling system. *International Journal of Heat and Mass Transfer, 44*(16), 3067–3080.

Rottman, J. W., & Simpson, J. E. (1983). Gravity currents produced by instantaneous release of a heavy fluid in a rectangular channel. *Journal of Fluid Mechanics, 135*, 95–110.

Sanders, J. E. (1965). Primary sedimentary structures formed by turbidity currents and related re-sedimentation mechanisms. In: G. V. Middleton (Ed.), *Primary sedimentary structures and their hydrodynamic interpretation – A symposium* (Vol. 12, pp. 192–219). Toronto: SEPM Spec. Publ.

Shin, J. O., Dalziel, S. B., & Linden, P. F. (2004). Gravity currents produced by lock exchange. *Journal of Fluid Mechanics, 521*, 1–34.

31 Simpson, J. E. (1999). *Gravity currents in the environment and the laboratory* (2nd ed.). Cambridge: Cambridge University Press.

Simpson, J. E., & Britter, R. E. (1979). The dynamics of the head of a gravity current advancing over a horizontal surface. *Journal of Fluid Mechanics, 94*(3), 477–491.

Thomas, L. P., Marino, B. M., & Linden, P. F. (1998). Gravity currents over porous substrate. *Journal of Fluid Mechanics, 366*, 239–258.

Yu, Y., Zhang, H., & Lemckert, C. J. (2014). Numerical analysis on the Brisbane River plume in Moreton Bay due to Queensland floods 2010–2011. *Journal of Environmental Fluid Mechanics, 14*(1), 1–24.

Zigic, S., King, B., & Lemckert, C. J. (2002). A study to investigate the mixing between two systems connected by an automated bi-directional gate structure. *Journal of Estuarine, Coastal and Shelf Science, 55*(1), 59–66.